LWT - Food Science and Technology 61 (2015) 407–413

Contents lists available at ScienceDirect

LWT - Food Science and Technology

journal homepage: www.elsevier.com/locate/lwt

Formulation and characterization of nanolaminated starch based film

Aníbal M. Slavutsky*, María A. Bertuzzi

Instituto de Investigaciones para la Industria Química (INIQUI-CONICET), CIUNSa, Facultad de Ingeniería, Universidad Nacional de Salta, Av. Bolivia 5150, A4408TVY, Salta, Argentina

ARTICLE INFO

Article history:
Received 16 July 2014
Received in revised form
26 November 2014
Accepted 15 December 2014
Available online 23 December 2014

Keywords:
Nanolaminated film
Sunflower oil
Sorption isotherm
Water barrier properties
Mechanical properties

ABSTRACT

Nanolaminated films were formulated by coating a hydrophilic film with a lipid nanolayer. This was performed by coating a starch film with sunflower oil, due to favourable interfacial forces that interact between the oil and the starch film support. The lipid nanolayer presence was corroborated by SEM analyses. Sorption isotherm curves of nanolaminated films show the same trend as starch films used as support but with an important reduction in the film water content through all the a_w range studied. The effect on permeability and diffusivity of the driving force (Δa_w) and a_w range, were evaluated. Water diffusion coefficients of oil laminated films are lower than the corresponding to starch films and in both cases, diffusivity decreases with a_w. Water vapour permeability depends on the driving force and a_w range, and it was concluded that in nanolaminated films, permeation phenomenon is controlled by water diffusion through the hydrophobic nanolayer. Nanolaminated films show an increase in tensile strength and Young module with a decrease in elongation in relation to starch based films.

1. Introduction

Edible films based on polysaccharides present suitable characteristics for food protection, but their functional properties are affected by humidity. However, the mechanical and water barrier properties of this promising material must be enhanced to compete with conventional petroleum-based polymers (Vieira, Da Silva, Dos Santos, & Beppu, 2011). Incorporation of nanofillers such as montmorillonite and cellulose nanocrystals has been studied as alternative to improve functional properties of starch based film (Slavutsky & Bertuzzi, 2012, 2014). Results indicated that improvements on functional properties of starch/montmorillonite nanocomposites films were dependent on the extent of nanoparticle dispersion into the starch matrix and the strength of interactions between starch chains and the nanofiller particles that reduce film affinity by water (Slavutsky & Bertuzzi, 2012).

Other alternative procedure used to improve the water barrier properties of hydrophilic films is to produce composite films by adding hydrophobic components such as lipids and waxes. A composite hydrocolloid-lipid film or coating has acceptable structural integrity imparted by the hydrocolloid and good water vapour barrier properties contributed by the lipid (Rhim & Shellhammer, 2005).

There are two types of composite films, according to their preparation method: emulsion or lamination. Emulsion based films are formulated by adding a lipid material and surfactants to a biopolymer solution. Drawbacks of emulsion films are related to the low lipid melting temperature, the solvent volatilization from the structural network, and the strong effect of emulsion droplet size and distribution, polarity, degree of saturation and polymorphism of lipid components on water barrier properties and mechanical properties of films and coatings (Pérez-Gago & Krochta, 2005).

Laminated films consist in a second distinguishable layer of hydrophobic lipid laminated over a preformed hydrophilic film, resulting in the lipid being a distinct layer within or atop the hydrophilic film. Their effect on mechanical properties is related to the characteristics of the hydrocolloid layer used and the moisture content of the films. Cracking and delamination frequently occur in bilayer films, ruining their excellent water barrier properties that depend on layer continuity. The preparation process requires two casting and drying steps and high temperature for lipid fusion or organic solvents for lipid dissolution (Pérez-Gago & Krochta, 2005). Nevertheless, bilayer films have 10–1000 times better barrier efficiency against water transfer than emulsified film (Debeaufort & Quezada-Gallo, 2000).

Mass transfer resistance of lipid compounds against gas and vapours migration is mainly due to their structure and hydrophobic character. When the crystals are dense, compact and

* Corresponding author. Tel.: +54 387 4255410; fax: +54 387 4251006.
E-mail address: amslavutsky@gmail.com (A.M. Slavutsky).

http://dx.doi.org/10.1016/j.lwt.2014.12.034
0023-6438/

homogeneously distributed, gas diffusion decreases, reducing gas permeability. On this basis, it may be assumed that the smaller the thickness of the lipid layer is, the more compact, crystalline and homogeneous lipid structure is achieved and then, the better barrier properties against water vapour are obtained in the laminated film.

A nanolaminated film consists of two or more layers of material with nanometric dimensions that are physically or chemically bonded to each other (Rubner, 2003). Multilayer films or coatings of nanometric thickness are usually made by successive adsorption of oppositely charged polyelectrolytes on a solid support. They can be used for potential applications such as food preservation and coatings (De S. Medeiros, Pinheiro, Carneiro-da-Cunha, & Vicente, 2012). However, the application of a lipid nanolayer onto a hydrocolloid film to obtain nanolaminated films has not been reported yet.

The aim of this work was to formulate and to characterize sunflower oil nanolaminated starch films (starch/SO) and to evaluate the effect of the lipid nanolayer on the functional properties of starch based films.

2. Materials and methods

2.1. Materials

Food grade corn starch (Unilever, Argentina) was used as polymeric matrix for film formulation. Food grade sunflower oil (SO) by Molinos Río de la Plata (Argentina) was used as lipid nanolayer. Glycerol (Mallinckrodt, USA) was added as plasticizer. Hexane was provided by Aldrich (USA). Ethylene glycol (Mallinckrodt, USA) was used for density determinations. P_2O_5 (Mallinckrodt, USA) was used as desiccant. All salts used to obtain the different relative humidity ambient (% RH) were provided by Aldrich (USA).

2.2. Film forming solution

Film forming dispersion consisted of 1 g of starch, 20 mL distilled water and 0.2 mL glycerol as plasticizer. The dispersion was gelatinized in a shaker water bath at 80 °C during 10 min. This procedure ensures the disintegration of starch granules to form a homogeneous solution. Starch solution, was cast over plastic dishes. Dishes were placed in an air-circulating oven at 35 °C until films were dry. After 15 h, dishes were removed from the oven and the films were peeled off. Isotropic and transparent films were obtained.

2.3. Preparation of nanolaminated films

The nanolaminated film (starch/SO) was composed of a lipid nanolayer on a starch film which acts as support. Starch films were previously stored at 53% RH for a week before the lipid nanolayer was added. Starch films were immersed into SO during 2 min, and subsequently rinsed with hexane. Afterwards, samples were kept in a chamber at 53% RH and 25 °C with air flow for 24 h, in order to eliminate the hexane. The effect of hexane on the starch film properties was studied through the same treatment on a starch film without the lipid nanolayer (SFC).

2.4. Characterization of nanolaminated films

2.4.1. Scanning electron microscopy (SEM)

Cross-sections and surface morphology of film samples were examined by SEM using a JEOL JSM 6480 LV scanning microscope (Boston, USA). Samples were previously stored in relative humidity controlled ambient during a week (53 %RH). Films were cryofractured by immersion in liquid nitrogen, before SEM observation. Samples were stored at 25 °C over silica gel. Film samples were mounted on bronze stubs and coated with gold. Samples were observed using an accelerating voltage of 15 kV.

2.4.2. Surface properties

In order to understand why an oil nanolayer (hydrophobic) in liquid state at the ambient temperature, is capable of adsorbing on the surface of a starch film (hydrophilic), a more detailed analysis of film surface properties was done. The analysis of polar and dispersive components of adhesion force was performed and the adhesion work (Wa) between the oil and the starch film was calculated. This study was based on the equations proposed by Clint and Wicks (2001) and Baldan (2012).

When a liquid of known surface tension is in static equilibrium with a solid surface, the relationship between the surface tensions is:

$$\gamma_S = \gamma_{SL} + \gamma_L \cos\theta \tag{1}$$

where γ_S is the surface tension of the solid substrate, γ_L is the surface tension of the liquid and γ_{SL} is the interfacial tension between the liquid and solid.

The affinity between the phases increases as the forces of attraction between different phases (bond strengths) are greater than the forces of attraction between molecules of the same phase (cohesive forces). The work of adhesion is defined as the energy per unit area required to separate two phases and is equal and opposite to the energy per unit area released when forming the interface. The work of cohesion (Wc) for a pure substance is the energy per unit area required to produce two new surfaces containing the same molecules. Increasing the surface is thermodynamically unfavourable process therefore is accompanied by an increase in Gibb's energy equal to the work to be delivered to the system to generate the increase in area.

The contact angle of a liquid on a surface is related to the work of adhesion, and can be calculated with the following equation:

$$Wa = \gamma_L(1 + \cos\theta) \tag{2}$$

The dispersive ($\gamma_L{}^d$) and polar ($\gamma_L{}^p$) components of the surface tension of a pure liquid are known and the contact angle (θ) between the solid surface and the liquid can be determined. The interactions can be described in terms of the work of adhesion (Wa):

$$Wa = W_a^d + W_a^p \Leftrightarrow Wa = 2\cdot\left(\sqrt{\gamma_S^d\cdot\gamma_L^d} + \sqrt{\gamma_S^p\cdot\gamma_L^p}\right) \tag{3}$$

where Wad and Wap are dispersive London forces and polar forces (acid–base interactions, for example) respectively and γSp and γSd are the polar and dispersive contributions to the solid surface under study. Replacing in Eq. (2) and rearranging yields:

$$\frac{1+\cos\theta}{2}\cdot\frac{\gamma_L}{\sqrt{\gamma_L^d}} = \sqrt{\gamma_S^p}\cdot\sqrt{\frac{\gamma_L^p}{\gamma_L^d}} + \sqrt{\gamma_S^d} \tag{4}$$

The Eq. (4) represents a straight line. The contact angle measured with different fluids was used to determine the independent variable $\sqrt{\gamma_L^p/\gamma_L^d}$ and the dependent variable $1+\cos\theta/2\cdot\gamma_L/\sqrt{\gamma_L^d}$, and from these values, the polar and dispersive components of the solid were obtained (Baldan, 2012; Clint & Wicks, 2001).

Gibb's energy was calculated through the following equation (Chaudhury, 1966):

$$\Delta G = W_c - 2\cdot\left(\sqrt{\gamma_S^d\cdot\gamma_L^d} + \sqrt{\gamma_S^p\cdot\gamma_L^p}\right) \quad (5)$$

Measurements of contact angles (θ) were performed by the sessile drop method at room temperature, using a goniometer (Standard Goniometer with DROP image standard, model 200-00, Ramé-Hart Instrument Co., Succasunna, USA). The contact angle measurements were performed with the following pure liquids: ethylene glycol, diiodomethane and ultra-pure water (Table 1). Five samples of each film formulation were tested. All tests were performed at time 0 in order to eliminate the anomalous behaviour of swelling.

2.5. Film density and thickness

Film samples of 3 cm × 3 cm were maintained in a desiccator with P_2O_5 (0% RH) for a week and weighed to determine the film density. Film density was calculated using Eq. (6),

$$\rho = \frac{m}{A\cdot\delta} \quad (6)$$

where A is the film area (9 cm^2), δ the film thickness (cm), m the film dry mass (g) and ρ the dry matter density of the film (g/cm^3). The film density was expressed as the average of five determinations. Film thicknesses were measured using an analogical thickness micrometer (Digimess, Buenos Aires, Argentina) at ten different points of the film to the nearest 0.001 mm. Test was performed in starch films, starch/SO films and SFC.

2.6. Moisture sorption isotherms

Constant relative humidity environments were established inside sorbostats (glass jars), using salt solutions. The salts used (LiBr, LiCl, CH_3COOK, $MgCl_2$, K_2CO_3, $Mg(NO_3)_2$, NaBr, NaCl, KCl) were the different salts recommended by the European project COST-90 (Spiess & Wolf, 1983), to cover a water activity (a_w) range from 0.05 to 0.90. A complete description of the followed methodology was previously described in Slavutsky and Bertuzzi (2012).

The moisture sorption determination was performed at 25 °C. Absorption tests were done in quadruplicate at each a_w.

Sorption data were fitted by BET and GAB models, described by Eqs. (7) and (8) respectively:

$$w_e = \frac{w_0\cdot C\cdot a_w}{(1-a_w)\cdot(1+(C-1)\cdot a_w)} \quad (7)$$

where w_e is the equilibrium moisture content (g water/100 g dry film), w_0 is the monolayer content (g water/100 g dry film), C is a temperature dependent adsorption constant.

$$w_e = \frac{w_0\cdot C\cdot k\cdot a_w}{(1-k\cdot a_w)\cdot(1-k\cdot a_w+C\cdot k\cdot a_w)} \quad (8)$$

Table 1
Surface tension[a] and contact angle between different liquids and starch films.

	Water	Ethylene glycol	Diiodomethane
γ_L (mN m^{-1})	72.10	47.7	50.8
γ_L^p (mN m^{-1})	59.20	17.6	2.3
γ_L^d (mN m^{-1})	19.90	30.1	48.5
Contact angle (°)	38.28 ± 1.03	46.03 ± 1.35	44.09 ± 0.93

[a] Data were extracted from Michalski et al. (1998).

Table 2
Mechanical properties, thickness and density of starch films, SFC films and starch/SO nanolaminated films.

	T (MPa)[a]	%E[a]	Y (MPa)[a]	Thickness (μm)[a]	ρ (g mL^{-1})
Starch	2.81 ± 1.0	44.91 ± 1.6	112 ± 9	91 ± 5	1.34 ± 0.07
Starch/SO	13.86 ± 1.3	11.03 ± 1.5	846 ± 11	91 ± 7	1.34 ± 0.09
SFC	2.59 ± 1.7	45.09 ± 1.9	111 ± 13	91 ± 6	1.34 ± 0.04

[a] Sample conditioned at 25 °C and 53% RH.

where w_e is the equilibrium moisture content (g water/100 g dry film), w_0 is the monolayer content (g water/100 g dry film), C is the Guggenhein constant, which is related to sorption heat monolayer, k is a correction factor that is referred to sorption heat multilayer (Eim, Rosselló, Femenia, & Simal, 2011).

The two models were compared by the statistical analysis of the extra sum-of-squares F technique. Test was performed in starch films and starch/SO films. SFC water content as a function of water activity was studied for a smaller number of a_w values (see Table 3).

2.7. Kinetics of water vapour sorption

The kinetic of water vapour sorption data were collected at 25 °C. Film samples (rectangular strips approximately 2 cm^2 area) were stored in a desiccator with P_2O_5 during a week. Afterwards, the samples were placed into an environmental chamber maintained at three different a_w (0.53, 0.76 and 0.91) using different salt solutions ($Mg(NO_3)_2$, NaBr and KCl). The samples were removed at specific intervals and weighted. The curves were fitted according to the Fick's diffusion equation for the one-dimensional diffusion of a solute into a sheet:

$$\frac{M_t}{M_\infty} = 1 - \frac{8}{\pi^2}\cdot\sum_{m=0}^{\infty}\frac{1}{(2\cdot m+1)^2}\,exp\left\{-D_0\cdot\frac{(2\cdot m+1)^2\pi^2\cdot t}{l^2}\right\} \quad (9)$$

where t is the time, l is film thickness, D_0 is the diffusion coefficient, M_t is the water uptake at time t and M_∞ is the water uptake at equilibrium value. The application of this equation is based on the assumption of a constant diffusion coefficient. Four samples of each film formulation were tested. Test was performed on starch films and starch/SO films.

2.8. Water vapour permeability

The apparatus and methodology described in ASTM E96 (ASTM, 2010a) were used to measure film permeability. Film specimens were conditioned during 72 h in a chamber at 25 °C and 53% RH ($Mg(NO_3)_2$ saturated salt solution) before being analysed. Films

Table 3
Moisture sorption data[a] of starch films, SFC films and Starch/SO films.[b]

a_w	Starch	SFC	Starch/SO
0.064	2.11 ± 0.86		0.64 ± 0.59
0.114	2.45 ± 0.56	2.03 ± 0.57	1.14 ± 0.60
0.237	3.51 ± 0.75		0.97 ± 0.95
0.329	4.59 ± 0.16	4.76 ± 0.77	1.22 ± 0.65
0.443	5.32 ± 1.18		2.23 ± 1.46
0.536	7.32 ± 0.28	7.84 ± 0.45	4.25 ± 1.23
0.653	11.62 ± 0.40		5.71 ± 0.41
0.762	17.11 ± 1.62	17.86 ± 0.79	10.88 ± 1.20
0.855	28.46 ± 0.96		20.69 ± 2.89
0.915	39.51 ± 0.84	38.28 ± 0.94	41.45 ± 0.69

[a] g water/100 g dry film.
[b] Data are the average of four tests. Standard deviations are indicated.

Table 4
BET and GAB model parameters of starch films and starch/SO films.

	Starch	Starch/SO
GAB		
w	5.657 ± 0.439	3.153 ± 0.378
c	2.420 ± 0.606	0.959 ± 0.349
k	0.947 ± 0.009	1.016 ± 0.007
R^2	0.9914	0.9911
$S_{y\cdot x}$[a]	1.158	1.221
BET		
w	3.631 ± 0.071	4.115 ± 0.134
C	17.81 ± 6.180	0.525 ± 0.083
R^2	0.9753	0.9904
$S_{y\cdot x}$	1.937	1.250

[a] Standard deviation of the residuals.

were sealed on cups containing different saturated salt solution, or distilled water that provides the highest relative humidity. Test cups were placed in a desiccator cabinet maintained at constant temperature. Saturated salt solutions or silica gel were used to generate specific relative humidity environments. In all cases, relative humidity inside the desiccator cabin (outside the cups) was lower than relative humidity inside the cups. Table 5 shows the driven force (Δa_w) used in each assay. A fan was used to maintain uniform conditions at all test locations over the specimen. Weight loss measurements were taken by continuous weighing of the test cup with an electronic scale to the nearest 0.001 g (Ohaus PA313, New York, USA). Data were transferred to a computer. Weight loss was plotted versus time and when steady state (straight line) was reached, 8 h more were registered. Thickness values used for water vapour permeability calculations were the mean value of five measurements. The water vapour transmission rate (WVTR) was calculated from the slope (G) of a linear regression of weight loss versus time (Eq. (10)) and measured water vapour permeability (P) was calculated according to Eq. (11):

$$WVTR = \frac{G}{A} \tag{10}$$

$$P = cte \cdot \frac{WVTR \cdot l}{(p_{w0} - p_{w2})} \tag{11}$$

where l is the film thickness; A is the area of exposed film, p_{w2} is partial pressure of water vapour at the film surface outside the cup (Pa), p_{w0} is the partial pressure of water vapour in the air at the surface of distilled water or saturated solution and cte is a constant to satisfy unit conversions.

Table 5
Water vapour permeability and WVTR of starch films, SFC and starch/SO films.

$a_w^{ext} - a_w^{int}$	$\lvert\Delta a_w\rvert$	Pc (g m^{-1} s^{-1} Pa^{-1})	WVTR (g day^{-1} m^{-2})
Starch			
0.000–1.000	1	9.08E-10 ± 19E-12	1498.60
0.329–0.536	0.207	7.14E-10 ± 19E-12	563.11
0.536–0.762	0.226	8.02E-10 ± 18E-12	486.61
0.762–1.000	0.238	1.88E-09 ± 25E-12	1282.89
0.329–0.762	0.433	5.03E-10 ± 27E-12	690.44
Starch/SO			
0.000–1.000	1	2.820E-10 ± 19E-12	910.16
0.329–0.536	0.207	4.881E-10 ± 25E-12	346.18
0.536–0.762	0.226	5.093E-10 ± 23E-12	386.88
0.762–1.000	0.238	9.111E-10 ± 20E-12	728.86
0.329–0.762	0.433	3.832E-10 ± 23E-12	562.94
SFC			
0.000–1.000	1	9.43E-10 ± 17E-12	1537.65

Corrected values of water vapour permeability (Pc) were obtained according the equations proposed by Gennadios, Weller, and Gooding (1994):

$$P_C = cte \cdot \frac{WVTR \cdot l}{(p_{w1} - p_{w2})} \tag{12}$$

p_{w1} is the partial pressure of water vapour at underside of films.

Test was carried out in triplicate for each type of film. Test was performed in starch films and starch/SO films for different driven forces (Δa_w). Permeability of SFC films was performed only for $\Delta a_w = 1$.

2.9. Mechanical properties

The tensile properties were measured using a texturometer Brookfield (Massachusetts, USA) according to ASTM D882 (ASTM, 2010b) with some modifications. The films were cut into strips of 25.4 mm wide and 80.0 mm long. The final film area exposed was 25.4 mm × 50.0 mm. The texturometer was set to tensile mode. Force and elongation were recorded during extension at 20 mm/min up to break. Before tension assay, all film strips were equilibrated during a week in a cabinet conditioned at 25 °C and 52% RH. The texturometer is placed in a chamber where the environmental conditions (temperature and % RH) are controlled. Five samples of each film formulation were tested. Elongation at break (%E), tensile strength (T) and Young's modulus (Y) were determined. Test was performed in starch films, starch/SO films and SFC.

3. Results and discussion

Starch/SO films were obtained by adsorption of an oil nanolayer on a starch film (see Section 2.3). Starch/SO films have a homogeneous, colourless, bright and transparent appearance, while starch films present a translucent and opaque aspect. Hexane was used to remove the remaining oil that was not adsorbed on the starch film surface. Starch films treated with hexane (SFC) did not present visual differences with untreated starch films.

Tables 2, 3 and 5 show the properties of starch films and SFC films studied. No significant differences were observed in the studied properties. This indicates that the immersion of starch films into hexane do not produce any modification on the starch film matrix. This could be due to the incompatibility between the solvent and the starch and the short immersion time.

3.1. Scanning electron microscopy

Fig. 1 shows the images obtained by SEM of starch films (Fig. 1a) and starch/SO nanolaminated films (Fig. 1b). Fig. 1c is a magnification of Fig. 1b (dual picture). A thin film deposited on starch film can be observed. These images confirm the construction of the nanolayered film on the starch film surface (indicated by an arrow in the Fig. 1b). The interface between the film and the nanolayer can be observed in the magnified image (Fig. 1c). The thickness of the deposited nanolayer is approximately 157 nm (±37). The nanolayer thickness was obtained with the software provided by the SEM equipment.

3.2. Surface properties

Table 1 shows the results of contact angle measurements. The best fitting parameters to the data set were obtained with a linear regression (Eq. (4)). Slope and the y-intercept, were used to determine polar and dispersive components of starch films:

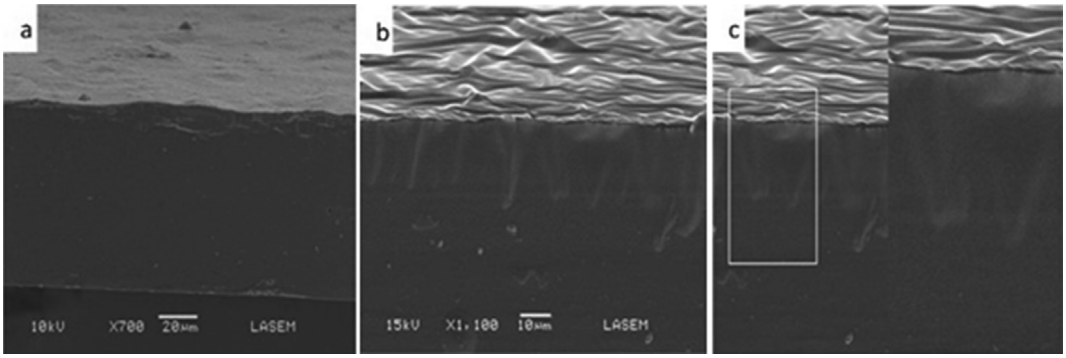

Fig. 1. SEM microphotographs of starch film and starch/SO films. (1.a starch film; 1.b starch/SO film; 1.c starch/SO film magnified).

$$\gamma_S^p = 36.10\frac{mN}{m}(\pm 0.78); \quad \gamma_S^d = 16.38\frac{mN}{m}(\pm 0.49)$$

These values indicate that starch films can interact with hydrophilic and hydrophobic substances. Similar results were obtained by Ghanbarzadeh et al. (2007) for zein proteins based films. Dispersive forces are nonpolar and weak attractions that operate in a relatively long range, more than 100 Å. Polar interactions are much stronger than the dispersive interactions, and they may act as short intervals as about 5 Å, and require intimate contact between the liquid and the solid surface (Wong, Gastineau, Gregorski, Tillin, & Pavlath, 1992). The adhesion between a solid and any substance involves intermolecular forces between the adhesive and the substrate, such as dipole–dipole interactions, Van der Waals forces and chemical interactions (i.e., ionic, covalent and metallic bonding). It is evident that the chemical bonds formed through the adhesive–substrate interface can greatly improve the grip between the two similar or dissimilar materials (substrates). These links are generally regarded as primary links compared to the physical interactions, such as Van der Waals, called secondary interactions strength. The distinction between primary and secondary link refers to the relative strength or binding energy of each type of interaction. The similarity of the dispersive and polar components between the liquid and a solid surface has a positive influence on the capacity of the liquid dispersion (Hershko & Nussinovitch, 1998). When polar and dispersive forces act in a short and large range, respectively, in most cases, a thin film on the solid surface will be adsorbed (Chaudhury, 1966). Therefore, the high dispersive component of starch films produces that oil molecules adhere to the film surface during the films immersion in the lipid. It can be concluded that the interaction between the two materials was mainly due to non-polar interactions.

The Wa is a measurement of the bond strength in a particular system. Polar and dispersive components on SO (Michalski, Desobry, Pons, & Hardy, 1998) were used to calculate Wa, with Eq. (3). The Wa obtained value was 51.50 mN m^{-1}. It indicates that SO adheres tenaciously to the film. This supports the strong adhesion between the starch film and SO that was observed in SEM images. Furthermore, due to the high Wa value, the washing with hexane removes only the oil portion that is not strongly adhered to the film. This explains why only a thin layer of nanometric size remains on the starch film surface. The Gibbs energy value calculated using Eq. (5) is negative ($\Delta G = -18.204$ mN m^{-1}), indicating that the adhesion between the oil and the film, is thermodynamically favourable.

The contact angle measurement is a useful tool to determine the hydrophobic or hydrophilic characteristics of a surface. The most wettable surfaces present low values ($\Theta < 20$) and the hydrophobic surfaces, on the contrary, show high values ($\Theta > 70$) of the contact angle. The wettability of a surface depends on the nature of the external layer in contact with the solvent. In the case of nanolaminated materials, the interpenetration of layers may cause some influence on that property (Fu, Ji, Yuan, & Shen, 2005), especially at the nanoscale. Contact angle value of Starch/SO nanlaminated film was 56.70 ± 1.15 and the determined for starch film was 38.28 ± 1.03 using water. Those values show that the lipid nanolayer reduces wettability of starch film increasing their water resistance.

3.3. Film density

Film density data are presented in Table 2. No significant differences between starch films, starch/SO films and SFC film were detected. It indicates that the nanolayer formation do not affect the film density. This could be explained by the very low amount of material incorporated onto the starch films.

3.4. Moisture sorption isotherms

Table 3 shows the sorption experimental data of starch films, SFC films and starch/SO films. Data indicates that the oil nanolayer formation on the starch film reduces the equilibrium moisture content of starch/SO films throughout all a_w range studied. Starch film and SCF do not present significant difference in moisture content throughout the a_w range studied. This indicates that the rinsing in hexane do not affect the microstructure and glycerol content of starch films.

Table 4 shows the best-fitting parameters of BET and GAB models calculated for the different film samples. The goodness of fit of both models was contrasted through the coefficient of determination R^2. Both models show a very good fit of all experimental data, however, GAB model presents a better fit of starch film data than BET model.

Moisture sorption data of starch film and starch/SO, as well as GAB model fitting, are shown in Fig. 2. The results indicate that the formation of the lipid nanolayer produces a decrease in the water sorption of starch films at lower and medium a_w ranges (0.0–0.7). At higher a_w values ($a_w > 0.7$) water sorption increases significantly for starch/SO films and both curves approximate. This increase in moisture content of systems formed by hydrophilic and hydrophobic substances, at high a_w values, has been studied by several authors. Morillon, Debeaufort, Blond, Capelle, and Voilley (2002) indicated that some hydrophobic substance containing hydrophilic groups, such as ester groups, carboxyl groups and hydroxyl groups, can be hydrated at high values of a_w. Donhowe and Fennema (1992) informed that water content of beeswax film increases exponentially at a_w around 0.8.

Monolayer values considerably decrease in nanolaminated films, approximately 40% of starch film value. The formation of the

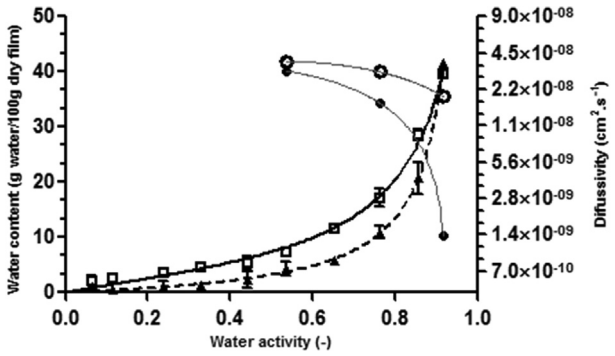

Fig. 2. Moisture sorption isotherms of starch films (□) and starch/SO films (▲), GAB model fit (starch —; starch/SO ····) and diffusion coefficient of starch films (○) and starch/SO films (●). Bars indicate standard deviation.

lipid nanolayer reduces the number of active sites where water molecules can interact over the film surface. The film moisture contents below a_w 0.7 are lower in starch/SO than starch films. Above this value, the moisture content exponentially increases in both cases, but water contents of starch/SO films are below of those corresponding to starch films.

3.5. Water vapour permeability and diffusivity

Permeant flow is proportional to the driving force for materials whose permeability is constant and not dependent on the permeant concentration in the material. However, data of Table 5 shows that the flux (WVTR) increases as the average moisture content of the film increases for a same value of the driving force. This is related to substantial modifications in the material that cause changes in its intensive properties such as permeability. The water vapour permeability is a combination of water solubility in the film and the diffusivity of water molecules in the starch matrix. Both phenomenological coefficients depend on moisture concentration in the polymer matrix. The nonlinearity of the water sorption isotherm shows the dependence of solubility with a_w. On the other hand, relaxation of the matrix structure with increasing moisture content alters the diffusion path of water molecules in the film. That is why the starch film permeability increases with a_w instead of being constant, and then the water vapour flow is not proportional to the imposed driving force. Morillon et al. (2002) reported for lipid materials that water permeability increases with the vapour pressure value when the same relative humidity gradient is established on the system. Table 5 shows Pc of starch films, starch/SO films and SFC films. It was observed that permeability of all samples is dependent on driving force (Δa_w). In addition, water permeability increases with a_w values at each side of the film when a similar Δa_w was used. The behaviour of starch films indicates that water molecules act plasticizing the film even at low relativity humidity gradient. Starch/SO films present lower permeability values than starch films throughout the range studied. This indicates that the lipid nanolayer reduce the affinity by water of starch based films used as support in starch/SO films. It is consistent with the lower water solubility in the film observed in the sorption isotherms of starch/SO films.

Phan The, Debeaufort, Voilley, and Luu (2009) incorporated hydrogenated vegetable fat by emulsion method into cassava starch and agar films and they studied its effect on permeability. Their results indicate that permeability increases with a_w range studied without significant differences with control films. Other authors obtained similar behaviour with gelatin/olive oil (Ma et al., 2012) and gelatin/sunflower oil (Pérez-Mateos, Montero, & Gómez-Guillén, 2009). It could be due the water permeation process occurs through the hydrophilic matrix and the lipid droplets act as fillers, generating an increase in the diffusive path.

Fig. 2 shows the calculated diffusion coefficient of starch and starch/SO films. Diffusivity values of starch films and starch/SO films decreases as a_w increases, when a_w values are higher than 0.5. This behaviour indicates that the increment in the film water content produces the relaxation of the polymer matrix and the progressive adsorption of water molecules in the generated active sites, producing a decrease of diffusivity coefficient (Slavutsky & Bertuzzi, 2012). Diffusivity values of starch/SO films are lower than those of starch films, because the deposited nanolayer on the starch film constitutes a hurdle on diffusion path of water molecules. Consequently, in the permeation process, the water molecules must overpass the nanolayer. Afterwards, the molecules diffuse through the film, and face against the barrier formed by the other nanolayer until they go through it up to the external environment. Probably, there is an accumulation of molecules between the film surface and the lipid nanolayer and the permeation phenomenon is controlled by the diffusion through the hydrophobic nanolayer.

3.6. Mechanical properties

Mechanical properties of starch films and starch/SO films are presented in Table 2. The experimental values show that the formation of the lipid nanolayer produces some changes on film mechanical properties. Starch/SO films evidence a large increase on tensile strength and Young module and a decrease on film elongation. These results can be correlated to the lower water content, according to sorption isotherm curves (Fig. 2). The water content of starch/SO films at 53% HR, is 60% lower than that corresponding to starch films. That difference on moisture content indicates that the film matrix of starch/SO is less plasticized and it could explain the mechanical behaviours of starch/SO films. Besides, according to Phan The, Debeaufort, Luu, and Voilley (2008), the lipid incorporation in hydrophilic films produced an antiplasticizing effect, which could reinforce the effect of the lower water content on the mechanical behaviour of the starch/SO film.

4. Conclusion

Nanolaminated films were formulated by coating starch films with a lipid nanolayer, driven by favourable interfacial forces that interact between oil molecules and the starch film. Owing to the low polar component value of SO, the adhesion between starch films and SO is determined by the affinity of dispersive components of both substances. The nanolayer formation was corroborated by SEM analyses. SEM images indicate that nanolayer presents a homogeneous thickness of nanoscale dimensions. This structure provides to the films better mechanical resistance with a large increase in Young module. Sorption isotherms indicate that starch/SO films reduce their affinity by water molecules at low and medium a_w range. Water molecules migrate during the permeation process generating the plasticizing and swelling of the starch matrix, even in starch/SO films. Water barrier properties were improved by the oil nanolayer deposition, probably due to the permeation phenomenon is controlled by the diffusion through the hydrophobic nanolayer. The proposed technique to elaborate nanolaminated films is simple, presents versatility and a great potential for the development of biodegradable packaging.

Acknowledgements

The financial support provided by CIUNSa de la Universidad Nacional de Salta (Proyecto N°1895/2) and by Agencia Nacional de Promoción Científica y Tecnológica (ANPCyT-IP-RPH 2007) are gratefully acknowledged. The authors thank technical assistance of LASEM (ANPCyT, CONICET, UNSA).

References

ASTM. (2010a). *E96. Standard test methods for water vapour transmission of materials*. Philadelphia: Standards American Society for Testing and Materials.

ASTM. (2010b). *D882 Standard test methods for tensile properties of thin plastic sheeting*. Philadelphia, USA: Standards American Society for Testing and Materials.

Baldan, A. (2012). Adhesion phenomena in bonded joints. *International Journal of Adhesion and Adhesives, 38*, 95–116.

Chaudhury, M. K. (1966). Interfacial interaction between low-energy surfaces. *Materials Science and Engineering, 16*, 97–159.

Clint, J. H., & Wicks, A. C. (2001). Adhesion under water: surface energy considerations. *International Journal of Adhesion and Adhesives, 21*(4), 267–273.

Debeaufort, F., & Quezada-Gallo, J. (2000). Lipid hydrophobicity and physical state effects on the properties of bilayer edible films. *Journal of Membrane Science, 180*, 47–55.

De S. Medeiros, B. G., Pinheiro, A. C., Carneiro-da-Cunha, M. G., & Vicente, A. A. (2012). Development and characterization of a nanomultilayer coating of pectin and chitosan. Evaluation of its gas barrier properties and application on "Tommy Atkins" mangoes. *Journal of Food Engineering, 110*(3), 457–464.

Donhowe, I. G., & Fennema, O. (1992). The effect of relative humidity gradient on water vapour permeance of lipid and lipid-hydrocolloid bilayer films. *Journal American Oil Chemistry Society, 69*, 1081–1087.

Eim, V. S., Rosselló, C., Femenia, A., & Simal, S. (2011). Moisture sorption isotherms and thermodynamic properties of carrot. *International Journal of Food Engineering, 7*(3), 1–18.

Fu, J., Ji, J., Yuan, W., & Shen, J. (2005). Construction of anti-adhesive and antibacterial multilayer films via layer-by-layer assembly of heparin and chitosan. *Biomaterials, 26*, 6684–6692.

Gennadios, A., Weller, C. L., & Gooding, C. H. (1994). Measurement errors in water vapour permeability of highly permeable, hydrophilic edible films. *Journal of Food Engineering, 21*(4), 395–409.

Ghanbarzadeh, B., Musavi, M., Oromiehie, A. R., Rezayi, K., Razmi Rad, E., & Milani, J. (2007). Effect of plasticizing sugars on water vapour permeability, surface energy and microstructure properties of zein films. *LWT – Food Science and Technology, 40*(7), 1191–1197.

Hershko, V., & Nussinovitch, A. (1998). The behaviour of hydrocolloid coatings on vegetative materials. *Biotechnology Progress, 14*(5), 756–765.

Ma, W., Chuan-He, T., Shou-Wei, Y., Xiao-Quan, Y., Qin, W., Fu, L., et al. (2012). Characterization of gelatin-based edible films incorporated with olive oil. *Food Research International, 49*(1), 572–579.

Michalski, M. C., Desobry, S., Pons, M. N., & Hardy, J. (1998). Adhesion of edible oils to food contact surfaces. *Journal of the American Oil Chemist's Society, 75*(4), 447–454.

Morillon, V., Debeaufort, F., Blond, G., Capelle, M., & Voilley, A. (2002). Factors affecting the moisture permeability of lipid-based edible films: a review. *Critical Reviews in Food Science and Nutrition, 42*(1), 67–89.

Pérez-Gago, M. B., & Krochta, J. M. (2005). Emulsion and bi-layer edible films. In J. H. Han (Ed.), *Innovations in food packaging* (pp. 384–402). New York: Elsevier Academic.

Pérez-Mateos, M., Montero, P., & Gómez-Guillén, M. C. (2009). Formulation and stability of biodegradable films made from cod gelatin and sunflower oil blends. *Food Hydrocolloids, 23*(1), 53–61.

Phan The, D., Debeaufort, F., Luu, D., & Voilley, A. (2008). Moisture barrier, wetting and mechanical properties of shellac/agar or shellac/cassava starch bilayer biomembrane for food applications. *Journal of Membrane Science, 325*(1), 277–283.

Phan The, D., Debeaufort, F., Voilley, A., & Luu, D. (2009). Influence of hydrocolloid nature on the structure and functional properties of emulsified edible films. *Food Hydrocolloids, 23*(3), 691–699.

Rhim, J. W., & Shellhammer, T. H. (2005). Lipid-based edible films and coatings. In J. H. Han (Ed.), *Innovations in food packaging* (pp. 362–383). New York: Elsevier Academic.

Rubner, M. F. (2003). pH-controlled fabrication of polyelectrolyte multilayers: assembly and applications. In G. Decher, & J. B. Schlenoff (Eds.), *Multilayer thin films: Sequential assembly of nanocomposite materials* (pp. 133–154). Deutsche: Weinheim Wiley-VCH.

Slavutsky, A. M., & Bertuzzi, M. A. (2012). A phenomenological and thermodynamic study of the water permeation process in corn starch/MMT films. *Carbohydrate Polymers, 90*(1), 551–557.

Slavutsky, A. M., & Bertuzzi, M. A. (2014). Water barrier properties of starch films reinforced with cellulose nanocrystals obtained from sugarcane bagasse. *Carbohydrate Polymers, 110*, 53–61.

Spiess, W. E. L., & Wolf, W. R. (1983). The results of the COST 90 project on water activity. In R. Jowitt, F. Escher, F. B. Hallstrom, M. F. Meffert, W. E. L. Spiess, & G. Vos (Eds.), *Physical properties of foods* (pp. 65–91). London: Applied Science.

Vieira, M. G. A., Da Silva, M. A., Dos Santos, L. O., & Beppu, M. M. (2011). Natural-based plasticizers and biopolymer films: a review. *European Polymer Journal, 47*(3), 254–263.

Wong, D. W. S., Gastineau, F. A., Gregorski, K. S., Tillin, S. J., & Pavlath, A. E. (1992). Chitosan-lipids films: microstructure and surface energy. *Journal of Agricultural and Food Chemistry, 40*(4), 540–544.